

Evaluation of the parenchymal distribution of renal steatosis in chronic kidney disease using chemical shift magnetic resonance imaging

Hüseyin Aydın^{1,A–F}, Hasan Aydın^{2,A,C,E,F}, Adnan Karabrahimoğlu^{3,A,C,E,F}, Baris Afsar^{4,C,E,F}

¹ Department of Radiology, Faculty of Medicine, Suleyman Demirel University, Isparta, Turkey

² Department of Radiology, Ankara Oncology Training and Research Hospital, University of Health Sciences, Turkey

³ Department of Biostatistics, Faculty of Medicine, Suleyman Demirel University, Isparta, Turkey

⁴ Department of Nephrology, Faculty of Medicine, Suleyman Demirel University, Isparta, Turkey

A – research concept and design; B – collection and/or assembly of data; C – data analysis and interpretation;

D – writing the article; E – critical revision of the article; F – final approval of the article

Advances in Clinical and Experimental Medicine, ISSN 1899–5276 (print), ISSN 2451–2680 (online)

Adv Clin Exp Med. 2024;33(5):455–462

Address for correspondence

Hüseyin Aydın

E-mail: huseyinrad@yahoo.com

Funding sources

None declared

Conflict of interest

None declared

Acknowledgements

The authors would like to thank Ozgur Pirgon (Professor, Department of Pediatric Endocrinology and Diabetes, Faculty of Medicine, Suleyman Demirel University, Isparta, Turkey) and Uğur Toprak (Professor, Department of Radiology, Faculty of Medicine, Eskişehir Osmangazi University, Turkey) for careful reading of the manuscript and helpful comments and suggestions.

Received on December 14, 2022

Reviewed on February 7, 2023

Accepted on May 25, 2023

Published online on June 21, 2023

Cite as

Aydın H, Aydın H, Karabrahimoğlu A, Afsar B. Evaluation of the parenchymal distribution of renal steatosis in chronic kidney disease using chemical shift magnetic resonance imaging. *Adv Clin Exp Med.* 2024;33(5):455–462. doi:10.17219/acem/166512

DOI

10.17219/acem/166512

Copyright

Copyright by Author(s)

This is an article distributed under the terms of the Creative Commons Attribution 3.0 Unported (CC BY 3.0) (<https://creativecommons.org/licenses/by/3.0/>)

Abstract

Background. Renal steatosis is an abnormal accumulation of fat in the kidney and may cause chronic kidney disease (CKD) or CKD progression.

Objectives. This pilot study aimed to evaluate the quantitative measurability of the parenchymal distribution of lipid deposition in the renal cortex and medulla using chemical shift magnetic resonance imaging (MRI) and investigate its relationship with clinical stages in CKD patients.

Materials and methods. The study groups included CKD patients with diabetes (CKD-d) (n = 42), CKD patients without diabetes (CKD-nd) (n = 31) and control subjects (n = 15), all of whom underwent a 1.5T MRI of the abdomen using the Dixon two-point method. The fat fraction (FF) values in the renal cortex and medulla were calculated from measurements made on Dixon sequences, and then compared between the groups.

Results. The cortical FF value was higher than the medullary FF value in control (0.057 (0.053–0.064) compared to 0.045 (0.039–0.052)), CKD-nd (0.066 (0.059–0.071) compared to 0.063 (0.054–0.071)), and CKD-d (0.081 (0.071–0.091) compared to 0.069 (0.061–0.077)) groups (all p < 0.001). The CKD-d group cortical FF values were higher than those of the CKD-nd group (p < 0.001). The FF values began increasing at CKD stages 2 and 3, and reached statistical significance at stages 4 and 5 in CKD patients (p < 0.001).

Conclusions. Renal parenchymal lipid deposition can be quantified separately in the cortex and medulla using chemical shift MRI. Fat accumulation occurred in cortical and medullary parenchyma in CKD patients, though predominantly in the cortex. This accumulation increased proportionally with the disease stage.

Key words: magnetic resonance imaging, chemical shift imaging, chronic kidney disease, renal steatosis, fatty kidney disease

Background

Renal steatosis is an abnormal accumulation of intracellular triglycerides/lipids in the kidney, which may cause the development and/or progression of chronic kidney disease (CKD).^{1–3} Fatty acids accumulate as intracellular droplets and cause the release of toxic cytokines, resulting in interstitial fibrosis and loss of kidney function.^{4–6} Inspired by non-alcoholic fatty liver disease (NAFLD), the term “fatty kidney disease (FKD)” has been used recently in the literature.⁶ In this regard, the effects of intra-abdominal, perirenal and parenchymal fat deposits on the kidneys are evaluated, as well as the relationships between FKD and insulin resistance, type 2 diabetes, obesity, metabolic syndrome, hyperlipidemia, hypertension, NAFLD, and cardiovascular disorders.^{6–8}

To evaluate renal steatosis, parenchymal lipid accumulation must be quantitatively measured. The gold standard renal steatosis assessment method is a biopsy followed by quantitative enzymatic measurement of triglycerides and qualitative oil red O staining. However, these methods are invasive and can increase the risk of complications.⁹ Non-invasive lipid measurement is also possible using fatty tissue-sensitive chemical shift magnetic resonance imaging (MRI).^{10–12} Chemical shift imaging is an MRI technique for detecting small areas (voxels) that contain water and fat protons. In this technique, the difference in resonance between water and oil protons is used to obtain images, with images taken from the in-phase (IP) and out-of-phase (OP) times of water and fat protons. In voxels containing both water and fat, signal loss occurs in OP images, though voxels containing only fat or water protons have no signal difference between the OP and IP images.¹³ With the simple addition and subtraction of the 2 images, 1 image containing only water and 1 containing only fat can be obtained. The Dixon technique can be generally used for the suppression or quantification of fat in various types of pulse sequences and allows for the measurement of the fat–water fraction in a precise region of interest (ROI) with higher spatial resolution.^{14,15} A few molecular imaging studies have recently evaluated lipid accumulation in the kidneys.^{7,11,12,15–17} However, no study has separately evaluated lipid deposition in the cortical and medullary components of the parenchyma.

Objectives

This pilot study evaluated the quantitative measurability of cortical and medullary parenchymal lipid deposition in CKD patients using chemical shift MRI.

Materials and methods

The study was carried out as a retrospective archive search. It was conducted in accordance with the Declaration of Helsinki after obtaining approval from the Clinical

Research Local Ethics Committee of the Faculty of Medicine of Suleyman Demirel University (Isparta, Turkey; decision No. 14/210 issues on July 27, 2020).

Study setting and participants

Study subjects were selected randomly from patients registered in the picture archiving and communication system (PACS) of our hospital, who were treated and followed up with a diagnosis of CKD and/or diabetes between 2016 and 2020, and those who had an upper abdominal MRI examination for any reason. In total, 117 CKD patients followed up in the Department of Nephrology were considered eligible for the study. Patients younger than 18 years ($n = 2$) or with malignancy ($n = 2$), polycystic or multicystic kidney disease ($n = 5$), renal transplantation ($n = 2$), or chronic liver disease ($n = 9$) were excluded from the study. Patients were also excluded if they had insufficient data in PACS ($n = 13$) or artifacts on MRI that prevented measurement ($n = 11$). The remaining 73 CKD patients were divided into 2 subgroups based on the presence or absence of diabetes, including CKD patients with diabetes (CKD-d) ($n = 31$) and CKD patients without diabetes (CKD-nd) ($n = 42$). The presence of diabetes was determined using the patient's history registered in the hospital PACS, the use of oral antidiabetic/insulin, or daily urine albumin level greater than 30 mg.¹⁸ The clinical staging of CKD was assigned according to the estimated glomerular filtration rate (eGFR),¹⁹ which was calculated using the CKD Epidemiology Collaboration (CKD-EPI) method.²⁰ The control group ($n = 15$) consisted of patients who underwent upper abdomen MRI for any reason other than kidney disease (such as liver hemangioma and gallbladder pathologies) and who, according to PACS data, did not have urinary disease, diabetes, malignancy, connective tissue disease, or chronic systemic disease. The final evaluation included 176 kidneys of 88 patients – 73 in the CKD group and 15 in the control group. All measurements required for fat fraction (FF) calculation from the renal cortical and medullary parenchyma were performed by a single radiologist (the corresponding author) with 10 years of abdominal MRI experience.

MRI examination parameters

Magnetic resonance imaging scans were obtained using a 1.5 Tesla unit (Magnetom Avanto; Siemens Medical Solutions, Erlangen, Germany) and a 16-channel body coil with the patient in supine position without sedation. Images were acquired as axial and coronal plane turbo spin-echo T2-weighted (TSE T2W) without fat saturation and breath-hold, and gradient-echo sequence fat saturated T1 volumetric interpolated breath-hold examination (VIBE), based on the Dixon two-point method and taken as IP and OP to detect intracellular lipid. The version of the VIBE-Dixon sequence applied in this study was a generic version

Table 1. Magnetic resonance examination parameters

Examination parameters	In-phase (IP)	Out-of-phase (OP)	Dixon Water (DW)	Dixon Fat (DF)
Voxel size [mm]	0.6 × 0.6 × 3	0.6 × 0.6 × 3	0.6 × 0.6 × 3	0.6 × 0.6 × 3
FOV [mm]	261 × 380	261 × 380	261 × 380	261 × 380
Matrix size [mm]	288 × 320	288 × 320	288 × 320	288 × 320
TR [ms]	7.08	7.08	7.1	7.1
TE [ms]	2.39	4.77	2.4	2.4
Flip angle [°]	10	10	10	10
Bandwidth [Hz/Px]	490	490	490	490
Slice thickness [mm]	3	3	3	3
NEX	1	1	1	1
Acquisition time [s]	16	16	16	16
Slice gap [mm]	20	20	20	20

FOV – field of view; TR – repetition time; TE – echo time; NEX – number of excitations.

rather than the modified quantitative Dixon sequence, so that IP, OP, water, fat, proton density fat fraction (PDFF), and T2* maps could be calculated. The chemical shift MRI examination parameters are presented in Table 1.

Evaluation of images and measurements

All images were evaluated using OsiriX MD v.10.0.2 software (General Public License (GPL) licensed free to access resource code and commercially licensed with US. Food and Drug Administration (FDA) approval; UCLA, Pixmeo, Bernex, Switzerland) on a MacOS-X radiology workstation (Apple Inc., Cupertino, USA). The measurements were performed by a single radiologist with 10 years of abdominal MRI experience. The intra-observer agreement values for measurements were found to be 0.918 (for cortical FF) and 0.956 (for medullary FF). Slices were evaluated on T2W images to exclude artifacts, space-occupying lesions or vascular pathologies. Measurements in the axial plane were made on Dixon Fat (DF) and Dixon Water (DW) sequences from the most appropriate single slice passing through the renal hilus level without any space-occupying lesions.

The ROI used for measurement in the DW sequence was placed using the copy–paste method in the same parenchymal location of the corresponding slice in the DF sequence so that the measurements were from the same location on both sequences, with the same ROI. Three measurements were taken using a 20-mm² circular ROI from the areas where the cortex and medulla meet, and then the average was calculated for analysis (Fig. 1). Renal FF values were calculated using the formula below¹³:

$$FF = [DF/(DF + DW)].$$

The sample size was found to be sufficient as a result of power analysis performed using the GPower 3.1.9.2 software (Kiel University, Kiel, Germany). The selected test family included F tests and fixed effects one-way analysis of variance (ANOVA). The effect size was calculated

as $d = 0.80$ using the measurements from the pilot study. The Type-I error rate and the power were considered 5% and 0.95, respectively. Therefore, the total sample size was determined as $n = 32$.

Statistical analyses

The statistical analyses employed IBM Statistical Package for Social Sciences (SPSS) v. 20.0 (IBM Corp., Armonk, USA) software. The continuous variables were expressed as mean with 95% confidence intervals (95% CIs), and the categorical variables as frequency (percentage (%)). The Shapiro–Wilk test assessed the normality of continuous variables. For comparisons between 2 independent groups, Student's t-test was applied with Welch robust correction test if the variances were not equal. One-way ANOVA with the Tamhane post hoc test was used for multiple groups since the variances were not homogenous, and the Brown–Forsythe robust correction test was applied to meet the assumptions of homogeneity. The receiver operating characteristic (ROC) analysis was performed, and the diagnostic ratios for sensitivity and specificity for cortical and medullary measurements were calculated. The intra-observer agreement was calculated using interclass correlation (ICC) with two-way mixed and average single-measure methods. There were no missing data in the dataset. A value of $p < 0.05$ was considered statistically significant.

Results

The evaluations included 176 kidneys of 88 adults (53.3% males, 46.7% females). The mean patient age was 59.28 ± 13.05 years in the CKD group and 55.41 ± 14.41 years in the control group ($p = 0.001$). Gender did not affect the FF values ($p > 0.05$).

The cortical FF values were significantly higher than the medullary FF in all groups ($p < 0.001$) (Table 2).

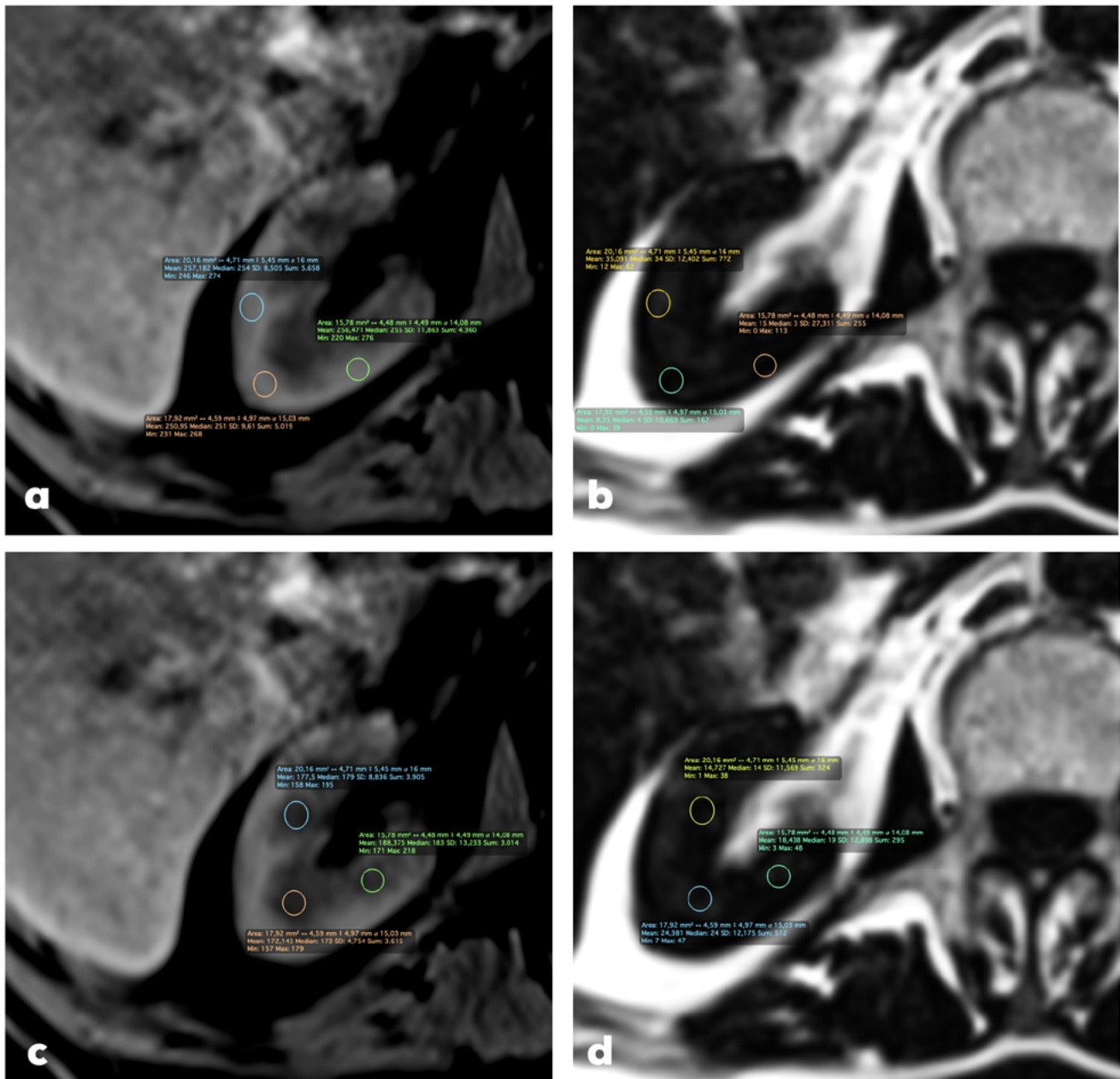


Fig. 1. Measurements recorded for Dixon Water (A) and Dixon Fat imaging (B) used to calculate cortical fat fraction (FF) values, and for Dixon Water (C) and Dixon Fat imaging (D) used to calculate medullary FF values

Table 2. Evaluation of the cortical and medullary distribution of renal lipid accumulation in the study groups

Study groups	n	Cortical FF	Medullary FF	Mean difference; t (Welch); df; p
		mean (95% CI)		
Control group	30	0.057 (0.053–0.064) ^a	0.045 (0.039–0.052) ^b	0.011; 5.022; 29; p < 0.001**
CKD patients	146	0.072 (0.064–0.078)	0.063 (0.054–0.071)	0.009; 4.103; 145; p < 0.001**
CKD without diabetic	84	0.066 (0.059–0.071)	0.058 (0.051–0.061)	0.007; 3.108; 83; p = 0.004**
CKD with diabetes	62	0.081 (0.071–0.091) ^a	0.069 (0.061–0.077) ^b	0.012; 3.172; 61; p = 0.002**
F_{contrast} ; df and p		5.081; df = 3 and p = 0.002*	6.753; df = 3 and p < 0.001*	–
Brown–Forsythe; df and p		10.444; df = 3 and p < 0.001*	78.435; df = 3 and p < 0.001*	–

* significant at p < 0.05 level according to one-way analysis of variance (ANOVA) with Brown–Forsythe robust correction test for heterogeneity of variances; H_0 – mean difference between the groups are the same; H_1 – at least 1 mean is different from other means; ** significant at p < 0.05 level according to t-test with Welch robust correction test for unequal variances; ^a the same superscript letters denote the significant pairwise comparison for the cortex fat fraction (FF) values between the study groups according to the Tamhane post hoc test; ^b the same symbols denote the significant pairwise comparison for the medullary FF values between the study groups according to the Tamhane post hoc test; CKD – chronic kidney disease; df – degrees of freedom; 95% CI – 95% confidence interval.

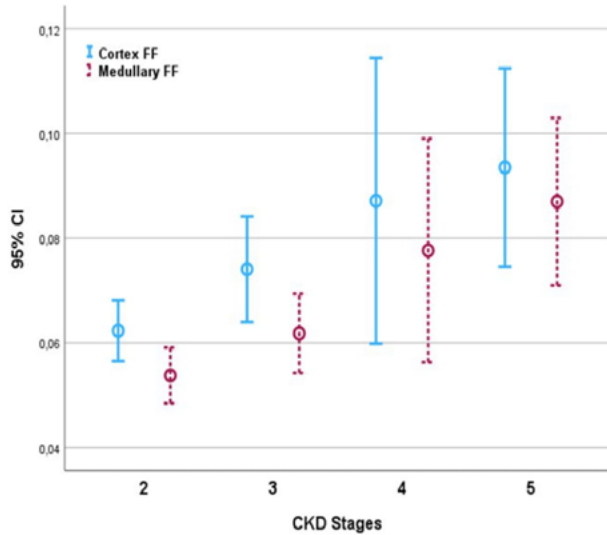


Fig. 2. Bar graph of the cortex and medulla fat fraction (FF) values with 95% confidence intervals (95% CIs) for chronic kidney disease (CKD) stages in all CKD patients (Brown–Forsythe = 3.817, degrees of freedom (df) = 3, 45.14; $p = 0.016$ for cortex FF with a significant Tamhane post hoc test result of comparison between stages 2 and 5 ($p = 0.021$); Brown–Forsythe = 6.318, $df = 3, 46.71$; $p = 0.001$ for medullary FF with a significant Tamhane post hoc test result of comparison between stages 2 and 5 ($p = 0.003$) and 3 and 5 ($p = 0.037$))

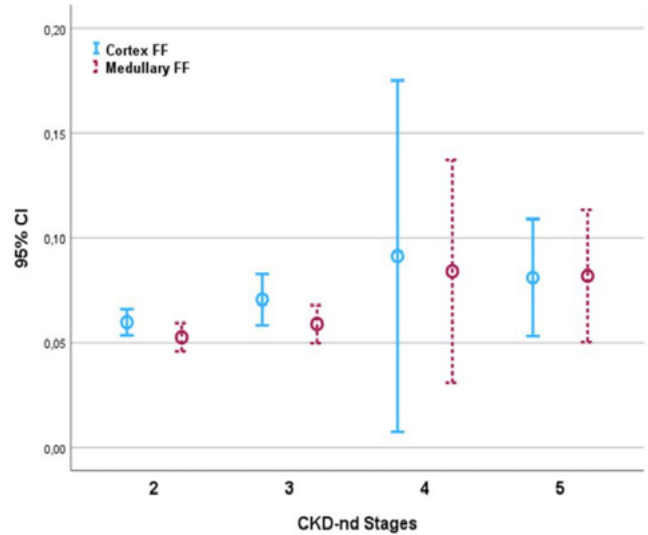


Fig. 4. Bar graph of the cortex and medulla fat fraction (FF) values with 95% confidence intervals (95% CIs) for chronic kidney disease (CKD) stages in non-diabetic chronic kidney disease (CKD-nd) patients (Brown–Forsythe = 2.954, degrees of freedom (df) = 3, 9.61; $p = 0.046$, for Cortex FF with significant a Tamhane post hoc test result of comparison between stages 2 and 5 ($p = 0.047$); Brown–Forsythe = 3.851, $df = 3, 12.83$; $p = 0.037$, for medullary FF with a significant Tamhane post hoc test result of comparison between stages 2 and 5 ($p = 0.040$))

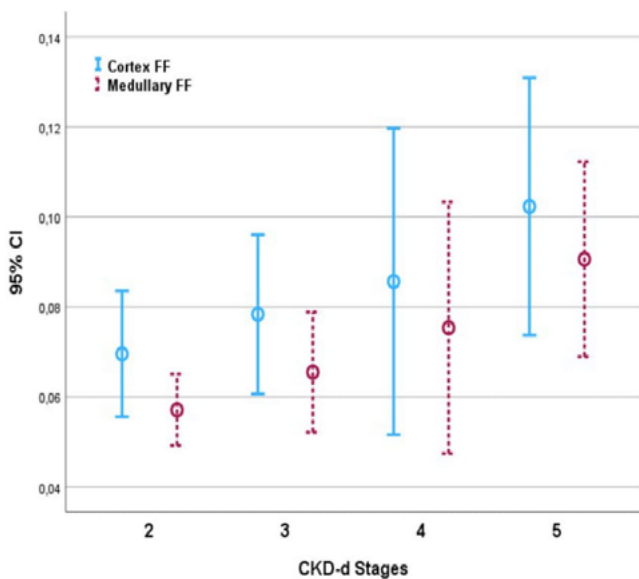


Fig. 3. Bar graph of the cortex and medulla fat fraction (FF) values with 95% confidence intervals (95% CIs) for chronic kidney disease (CKD) stages in diabetic chronic kidney disease (CKD-d) patients (Brown–Forsythe = 3.428, degrees of freedom (df) = 3, 34.73; $p = 0.038$, for Cortex FF with a significant Tamhane post hoc test result of comparison between stages 2 and 5 ($p = 0.037$); Brown–Forsythe = 4.634, $df = 3, 30.03$; $p = 0.043$, for medullary FF with a significant Tamhane post hoc test result of comparison between stages 2 and 5 ($p = 0.041$))

In the CKD-d patients, a significant increase was observed in the cortical FF values compared to the control subjects ($p < 0.001$). The medullary FF values in both CKD groups increased, but the values were significantly higher in the CKD-d group than in the control group ($p < 0.001$). However, in contrast to the CKD-d group, the elevated cortical and medullary FF values in the CKD-nd group

had no statistical significance compared to the control group ($p > 0.05$).

The cortical and medullary FF measurements in the CKD groups, based on the CKD stages, are presented in Fig. 2–4. There was no significant difference between the control group (healthy kidneys) and the CKD groups at stage 1 for cortical and medullary FF values ($p > 0.05$). When all CKD patients were considered as a single group, there was no significant difference between stage 1 and 2 cortical FF values. A statistically significant difference was determined in the cortical and medullary FF values at stage 2 compared to stage 5 values (cortex, $p = 0.021$; medulla, $p = 0.003$). In addition, there was a significant difference between stage 3 and stage 5 for medulla values ($p = 0.037$) (Fig. 2). In the CKD-d group, the cortical and medullary FF values increased with the clinical stage and reached statistical significance between stages 2 and 5 ($p = 0.037$ and $p = 0.041$, respectively) (Fig. 3). The cortical and medullary FF values in the CKD-nd group were similar to those of the CKD-d group, with statistical significance between stages 2 and 5 (cortex, $p = 0.047$; medulla, $p = 0.040$) (Fig. 4).

The ROC analysis showed a significant difference between the control and CKD-d patient groups with respect to the area under the curve (AUC) values for both cortical and medullary FF. The cutoff value of 0.076 for cortical FF had a sensitivity of 96.7%, while the cutoff value of 0.056 for medullary FF had better diagnostic ratios, as shown in Table 3.

The results of normality and homogeneity of variance assumptions with related tests are presented in Supplementary Table 1 (<https://doi.org/10.5281/zenodo.7961812>).

Table 3. Receiver operating characteristic (ROC) analysis results of cortical and medullary fat fraction (FF) values between the control group and diabetic chronic kidney disease (CKD-d) patients

FF measurements	Comparison group 1	Comparison group 2	AUC (95% CI)	p-value	Cutoff value	Sensitivity [%] (95% CI)	Specificity [%] (95% CI)
Cortical FF	control	CKD-d	0.699 (0.591–0.806)	0.002*	0.076	96.7 (91.05–99.24)	39.0 (29.40–49.27)
Medullary FF	control	CKD-d	0.768 (0.670–0.866)	<0.001*	0.056	83.3 (74.52–90.01)	61.7 (51.44–71.25)

* significant at 0.05 level according to ROC analysis; AUC – area under curve; 95% CI – 95% confidence interval.

Discussion

This study demonstrated for the first time the separate quantitative evaluation of parenchymal lipid deposition in the cortex and medulla and its relationship with the clinical stages of CKD using a radiological imaging method. We found that fat accumulation occurs in the cortex and medulla in CKD patients, predominantly in the cortex, and is positively correlated with the clinical stages of CKD. The importance of lipid accumulation in the cortex relative to the medulla in the early stages of diabetes demonstrated using MRI was consistent with the biopsy findings, suggesting that this technique is valid for measuring cortical and medullary lipid accumulation in the kidney. Previous histopathological studies have shown that parenchymal intracellular lipid deposition in CKD mainly occurs in the parts of the renal cortex containing the glomerulus and proximal tubules.^{21,22} Magnetic resonance imaging studies have demonstrated the presence of very little renal parenchymal lipid in healthy volunteers and an increase in the amount of lipid in the kidney parenchyma (without cortex/medulla distinction) in diabetic patients.^{11,17,23} However, as far as we know, an MRI study on the distribution of parenchymal lipid deposition in the cortex and medullary components in CKD patients, as well as on its relationship with clinical stages, has not yet been performed.

Cortical and medullary lipid depositions differed according to the CKD stage.^{24,25} At stage 1 CKD, there was no significant increase in the amount of parenchymal lipid, and the cortical and medullary lipid distributions were similar to those of the control group. In CKD patients, parenchymal lipids increased from stage 2 and reached a statistically significant level at stages 4 and 5. Although there was no statistical significance at stages 2 and 3, the FF increase was greater in the cortex than in the medulla. There was no significant difference between the cortex and medulla in lipid accumulation at stages 4 and 5, which suggests that parenchymal lipid accumulation is diffuse in advanced CKD. The detection of different amounts of lipid accumulation in parenchymal components in different clinical stages suggests that this novel technique presents a new area of research for experimental clinical and drug studies. If the technique proves useful, it can be applied free of charge to patients undergoing MRI for any reason, since chemical shift sequences are routinely obtained during abdominal MRI scans. In this regard, prospective multicenter studies can be conducted with larger patient groups to determine

cutoff values according to the clinical stages of CKD and test inter-observer and intra-observer reliability.

Renal lipid accumulation may develop independently of hyperglyceridemia.⁶ In the CKD-nd group, cortical and medullary FF values increased in parallel with the increase in the clinical stage, but no statistical significance was identified (Table 2). The possible reason for this discrepancy may be the lower number of stage 4 and 5 CKD patients in this group compared to those at stages 1 and 2.

The relationship between diabetes and renal parenchymal lipid accumulation is not clear. Some studies have reported that diabetes does not have a significant relationship with renal lipid accumulation.^{22,24} In contrast, other studies have reported a significant increase of renal lipid content in diabetes patients.^{11,17,23} Yokoo et al. conducted a study using 3T MRI, with measurements taken from an ROI through the whole parenchyma, and reported that the renal parenchyma FF rate (2.38%) was high in diabetes patients, independently of serum creatinine, body mass index (BMI) and Hb-A1c, and concluded that steatosis was an independent risk factor.¹¹ In the present study, the increase in FF values in CKD-d group was higher than in the CKD-nd group, and the cortical and medullary FF values increased in parallel with the increasing stage. This finding suggests that diabetes could have a triggering effect on lipid accumulation in patients with CKD. However, it would not be correct to make a conclusion regarding the impact of diabetes on renal steatosis based on the results of the current study. Indeed, this study only focused on measuring FF in the renal cortex and medulla in CKD, and there was no evaluation of other risk factors that may affect renal steatosis, such as diabetes severity and duration, concomitant hypertension, metabolic syndrome, or obesity.

Inspired by the concept of NAFLD, the term FKD has recently been proposed to express the local and systemic effects of ectopic fat accumulation. Within this concept, the renal effects of intra-abdominal, perirenal and parenchymal fat depositions are evaluated (albuminuria, CKD, and podocyte toxicity).⁷ Thus, as for NAFLD, it has been reported that renal steatosis can be treated as a separate disease or can be a part of a more extended metabolic disorder.^{6,7} Such a distinction is important for clinical purposes, and targeting metabolic disorders as a whole may also impact kidney structure and function. In this regard, it is crucial to evaluate if the medications for NAFLD can also decrease kidney lipid accumulation.⁸ Moreover, it is clinically important to investigate the relative impact of cortical

or medullary lipid accumulation. As this pilot study primarily aimed to measure fat accumulation quantitatively in the cortex and medulla but not to investigate the clinical significance of cortical and medullary fat accumulation, future studies are needed to highlight these issues. However, in contrast to NAFLD, in which fat accumulation is clearly evident, lipid accumulation in the kidney is scarce and sensitive techniques may be necessary to evaluate trace amounts of fat deposition, which may be clinically important.

Multiparametric renal MRI biomarkers have been developed and proposed for evaluating renal inflammation, oxidative stress, hypoxia, and fibrosis.^{26,27} However, a standard radiological approach that will contribute to the definition of FKD has not yet been developed.⁷ The present study showed that the addition of quantitative parenchymal FF measurements using chemical shift renal MRI could contribute to FKD understanding and development, though more studies are required to highlight the clinical importance of our findings.

Limitations

This study had several limitations. Selection bias is inherent to the retrospective design of the study. Although biopsy is the gold standard, it was not performed to measure the amount of fat in the renal parenchyma. However, the chemical shift MRI technique, which is accepted for assessing lipids in the liver, was used for the noninvasive measurement of the amount of renal parenchymal lipids. The diagnosis and staging of CKD were defined according to eGFR, though there is an increasing recognition that eGFR alone may not be specific to CKD, and the Kidney Disease: Improving Global Outcomes (KDIGO) recommendations suggest adding proteinuria to the classification.²⁶ Moreover, the study focused on quantifying fat accumulation in the renal cortex and medulla in patients with CKD and evaluating its relationship with the clinical stage. However, it may be interesting to investigate the relationship between renal parenchymal steatosis and parameters such as obesity, hypertension, metabolic syndrome, uric acid, insulin resistance, triglycerides, fasting blood glucose, and hemoglobin A1C (HbA1c) using this method. Also, the reliability of the measurements could not be evaluated, as they were made by a single observer. However, the measurements were reliable since the cortex and medulla are clearly distinguished in Dixon Water images, measurements are made from the same section and region with the cut–copy–paste technique, and the number and size of the measurements are standard.

Conclusions

Results of this study demonstrated that fat accumulation occurred in both the cortex and medulla, predominantly in the cortex of CKD patients, and correlated positively with the clinical stages of CKD. As such, FF measurements

using chemical shift MRI could be used as a radiological criterion for developing the FKD concept, since even very small cortical and medullary lipid deposits can be measured quantitatively. However, to validate these findings, there is a need for prospective multicenter trials with larger patient groups to determine cutoff values and test intra-observer and inter-observer reliabilities according to the clinical stages of CKD.

Supplementary data

The supplementary materials are available at <https://doi.org/10.5281/zenodo.7961812>. The package contains the following files:

Supplementary Table 1. The results of normality and variance homogeneity assumptions.

ORCID iDs

Hüseyin Aydın  <https://orcid.org/0000-0003-4704-4759>

Hasan Aydın  <https://orcid.org/0000-0002-8038-7035>

Adnan Karabrahimoğlu  <https://orcid.org/0000-0002-8277-0281>

Baris Afsar  <https://orcid.org/0000-0002-1369-3657>

References

- Escasany E, Izquierdo-Lahuerta A, Medina-Gomez G. Underlying mechanisms of renal lipotoxicity in obesity. *Nephron*. 2019;143(1):28–32. doi:10.1159/000494694
- Garofalo C, Borrelli S, Minutolo R, Chiodini P, De Nicola L, Conte G. A systematic review and meta-analysis suggests obesity predicts onset of chronic kidney disease in the general population. *Kidney Int*. 2017;91(5):1224–1235. doi:10.1016/j.kint.2016.12.013
- Foster MC, Hwang SJ, Porter SA, Massaro JM, Hoffmann U, Fox CS. Fatty kidney, hypertension, and chronic kidney disease: The Framingham Heart Study. *Hypertension*. 2011;58(5):784–790. doi:10.1161/HYPERTENSIONAHA.111.175315
- Restini CBA, Ismail A, Kumar RK, et al. Renal perivascular adipose tissue: Form and function. *Vasc Pharmacol*. 2018;106:37–45. doi:10.1016/j.vph.2018.02.004
- Simon N, Hertig A. Alteration of fatty acid oxidation in tubular epithelial cells: From acute kidney injury to renal fibrogenesis. *Front Med (Lausanne)*. 2015;2:52. doi:10.3389/fmed.2015.00052
- Mende CW, Einhorn D. Fatty kidney disease: A new renal and endocrine clinical entity? Describing the role of the kidney in obesity, metabolic syndrome, and type 2 diabetes. *Endocrine Pract*. 2019;25(8):854–858. doi:10.4158/EP-2018-0568
- Mende C, Einhorn D. Fatty kidney disease: The importance of ectopic fat deposition and the potential value of imaging. *J Diabetes*. 2022;14(1):73–78. doi:10.1111/1753-0407.13232
- Byrne CD, Targher G. NAFLD as a driver of chronic kidney disease. *J Hepatol*. 2020;72(4):785–801. doi:10.1016/j.jhep.2020.01.013
- Bobulescu IA. Renal lipid metabolism and lipotoxicity. *Curr Opin Nephrol Hypertens*. 2010;19(4):393–402. doi:10.1097/MNH.0b013e32833aa4ac
- Pacifico L, Nobili V, Anania C, Verdecchia P, Chiesa C. Pediatric nonalcoholic fatty liver disease, metabolic syndrome and cardiovascular risk. *World J Gastroenterol*. 2011;17(26):3082–3091. doi:10.3748/wjg.v17.i26.3082
- Yokoo T, Clark HR, Pedrosa I, et al. Quantification of renal steatosis in type II diabetes mellitus using dixon-based MRI. *J Magn Reson Imaging*. 2016;44(5):1312–1319. doi:10.1002/jmri.25252
- Klinkhammer BM, Lammers T, Mottaghy FM, Kiessling F, Floege J, Boor P. Non-invasive molecular imaging of kidney diseases. *Nat Rev Nephrol*. 2021;17(10):688–703. doi:10.1038/s41581-021-00440-4
- Dixon WT. Simple proton spectroscopic imaging. *Radiology*. 1984;153(1):189–194. doi:10.1148/radiology.153.1.6089263
- Lins CF, Salmon CEG, Nogueira-Barbosa MH. Applications of the Dixon technique in the evaluation of the musculoskeletal system. *Radiol Bras*. 2021;54(1):33–42. doi:10.1590/0100-3984.2019.0086

15. Jonker JT, De Heer P, Engelse MA, et al. Metabolic imaging of fatty kidney in diabetes: Validation and dietary intervention. *Nephrol Dial Transplant*. 2018;33(2):224–230. doi:10.1093/ndt/gfx243
16. Dekkers IA, De Heer P, Bizino MB, De Vries APJ, Lamb HJ. ¹H-MRS for the assessment of renal triglyceride content in humans at 3T: A primer and reproducibility study. *J Magn Reson Imaging*. 2018;48(2):507–513. doi:10.1002/jmri.26003
17. Sijens PE. MRI-determined fat content of human liver, pancreas and kidney. *World J Gastroenterol*. 2010;16(16):1993. doi:10.3748/wjg.v16.i16.1993
18. Kidney Disease: Improving Global Outcomes (KDIGO) CKD Work Group. Notice: KDIGO 2012 clinical practice guideline for the evaluation and management of chronic kidney disease. *Kidney Int Suppl*. 2013;3(1):1. doi:10.1038/kisup.2012.73
19. Kidney Disease: Improving Global Outcomes (KDIGO) CKD-MBD Work Group. KDIGO clinical practice guideline for the diagnosis, evaluation, prevention, and treatment of chronic kidney disease—mineral and bone disorder (CKD-MBD). *Kidney Int Suppl*. 2009;76(Suppl 113):S1–S2. doi:10.1038/ki.2009.188
20. Florkowski CM, Chew-Harris JS. Methods of estimating GFR: Different equations including CKD-EPI. *Clin Biochem Rev*. 2011;32(2):75–79. PMID:21611080.
21. Kim JJ, Wilbon SS, Fornoni A. Podocyte lipotoxicity in CKD. *Kidney360*. 2021;2(4):755–762. doi:10.34067/KID.0006152020
22. Bobulescu IA, Lotan Y, Zhang J, et al. Triglycerides in the human kidney cortex: Relationship with body size. *PLoS One*. 2014;9(8):e101285. doi:10.1371/journal.pone.0101285
23. Hammer S, De Vries APJ, De Heer P, et al. Metabolic imaging of human kidney triglyceride content: Reproducibility of proton magnetic resonance spectroscopy. *PLoS One*. 2013;8(4):e62209. doi:10.1371/journal.pone.0062209
24. Wang YC, Feng Y, Lu CQ, Ju S. Renal fat fraction and diffusion tensor imaging in patients with early-stage diabetic nephropathy. *Eur Radiol*. 2018;28(8):3326–3334. doi:10.1007/s00330-017-5298-6
25. Gai Z, Wang T, Visentin M, Kullak-Ublick G, Fu X, Wang Z. Lipid accumulation and chronic kidney disease. *Nutrients*. 2019;11(4):722. doi:10.3390/nu11040722
26. Selby NM, Blankestijn PJ, Boor P, et al. Magnetic resonance imaging biomarkers for chronic kidney disease: A position paper from the European Cooperation in Science and Technology Action PARENCHIMA. *Nephrol Dial Transplant*. 2018;33(Suppl 2):ii4–ii14. doi:10.1093/ndt/gfy152
27. Pruijm M, Mendichovszky IA, Liss P, et al. Renal blood oxygenation level-dependent magnetic resonance imaging to measure renal tissue oxygenation: A statement paper and systematic review. *Nephrol Dial Transplant*. 2018;33(Suppl 2):ii22–ii28. doi:10.1093/ndt/gfy243